Room-Temperature Molten Salts of Ruthenium Tris(bipyridine)

Hitoshi Masui and Royce W. Murray*

Kenan Laboratories of Chemistry, The University of North Carolina, Chapel Hill, North Carolina 27599-3290

Received May 22, 1997[⊗]

Attaching poly(ethylene glycol)−mono(methyl ether) (MW 350) chains to $[Ru(bpy)_3]^{2+}$ complexes via 4,4′-bipyridine ester linkages produces room temperature, highly viscous, molten salt forms of this well-known complex. This paper describes the synthesis and properties of a series of such complexes bearing two, four, or six polyether chains. Differential scanning calorimetry, rheometry, microelectrode voltammetry, and ac impedance spectroscopy were used to determine the dependence of physical and transport properties of the Ru complex melts on the number of polyether tails. The coupling of electron hopping and physical diffusion in voltammetrically generated mixed-valent layers is analyzed using the Dahms−Ruff relationship, yielding self-exchange rate constants, k_{ex}, for the Ru(III/II) and Ru(II/I) couples. An activation analysis shows that these reactions are adiabatic, or nearly so, and the slowing of their rates relative to that of the parent $[Ru(bpy)_3]^{2+}$ complex in fluid solutions is caused by large thermal barriers.

Interest in the electrochemistry and electron transfer chemistry of redox-active species in viscous, glassy, and solid state media has led us to explore new redox-active compounds which are room-temperature viscous liquids. These materials are based upon attaching short poly(ethylene glycol)−mono(methyl ether) (MePEG) chains to a target redox compound,[1] transforming it from its usual crystalline habit into a melt and, typically, a glass former. They can be regarded as *hybrid* redox polyethers. Such readily processible substances have potential usefulness in electrochromic and electroluminescent displays,[2] molecular electronic devices,[3] and polymer electrolytes and batteries.[4]

This paper presents the synthesis of the first examples of room-temperature molten salt forms of the famous ruthenium tris(bipyridine) complex as the derivatives $[Ru(bpy)_N(bpy(CO_2\text{-MePEG-350})_2)_{3-N}](ClO_4)_2$, where $N = 0$, 1, and 2. These new "tailed" complexes (Chart 1) are, for obvious reasons, abbreviated as the 2-tail complex ($N = 2$), the 4-tail complex ($N = 1$), and the 6-tail complex ($N = 0$).

Chart 1. Molecular Structures and Nomenclature

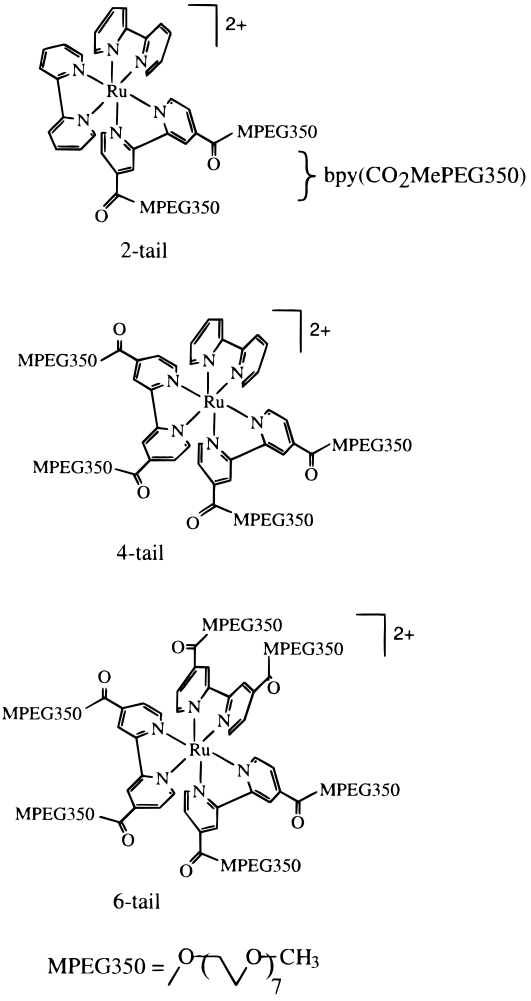

As part of a project[1,3a,5] on the effects of constrained (near-solid) environments on electron transfer dynamics and mass transport in redox materials, we have measured ionic conductivities and diffusion coefficients of the three *undiluted* Ru

[⊗] Abstract published in *Advance ACS Abstracts,* October 1, 1997.

(1) (a) Velazquez, C. S.; Hutchison, J. E.; Murray, R. W. *J. Am. Chem. Soc.* **1993**, *115*, 7896. (b) Hatazawa, T.; Terrill, R. H.; Murray, R. W. *Anal. Chem.* **1996**, *68*, 597. (c) Poupart, M. W.; Velazquez, C. S.; Hassett, K; Porat, Z.; Haas, O.; Terrill, R. H.; Murray, R. W. *J. Am. Chem. Soc.* **1994**, *116*, 1165. (d) Terrill, R. H.; Hatazawa, T.; Murray, R. W. *J. Phys. Chem.* **1995**, *99*, 16676. (e) Velazquez, C. S.; Murray, R. W. *J. Electroanal. Chem.* **1995**, *396*, 349. (f) Long, J. W.; Velazquez, C. S.; Murray, R. W. *J. Phys. Chem.* **1996**, *100*, 5492. (g) Williams, M. E.; Long, J. W.; Masui, H.; Murray, R. W. *J. Am. Chem. Soc.* **1997**, *119*, 1997. (h) Terrill, R. H.; Hutchison, J. E.; Murray, R. W. *J. Phys. Chem.* **1997**, *101*, 1535. (i) Emmenegger, F.; Williams, M. E.; Murray, R. W. *Inorg. Chem.* **1997**, *36*, 3146. (j) Williams, M. E.; Lyons, L. J.; Long, J. W.; Murray, R. W. *J. Phys. Chem.*, in press.

(2) (a) Pei, Q.; Gang. Y.; Zhang, C.; Yang, Y.; Heeger, A. J. *Science* **1995**, *269*, 1086. (b) Maness, K. M.; Terrill, R. H.; Meyer; T. J.; Murray, R. W.; Wightman, R. M. *J. Am. Chem. Soc.* **1996**, *118*, 10609. (c) Maness, K. M.; Masui, H.; Wightman, R. M.; Murray, R. W. *J. Am. Chem. Soc.* **1997**, *119*, 3987.

(3) (a) Terrill, R. H.; Murray, R. W. In *Molecular Electronics*; Jortner, J., Ratner, M. A., Eds.; IUPAC Series Chemistry for the 21st Century; Blackwell Science: Oxford, U.K.; in press. (b) Buck, R. P.; Surridge, N. A.; Murray, R. W. *J. Electrochem. Soc.* **1992**, *139*, 136. (c) Miller, J. S. *Adv. Mater.* **1990**, *378*, 495. (d) Kido, J.; Kimura, M.; Nagai, K. *Science* **1995**, *267*, 1332. (e) Kemp, M.; Roitberg, A.; Mujica, V.; Wanta, T.; Ratner, M. A. *J. Phys. Chem.* **1996**, *100*, 8349. (f) Barbara, P. F.; Meyer, T. J.; Ratner, M. A. *J. Phys. Chem.* **1996**, *100*, 13148.

(4) (a) MacCallum, J. R.; Vincent, C. A. Eds., *Polymer Electrolyte Reviews−1 and 2*; Elsevier Applied Science: London, 1987 and 1989. (b) Gauthier, M. Fauteaux, D.; Vassort, G.; Belanger, A.; Duval, M.; Ricouxi, P.; Chabagno, J.-M.; Muller, D.; Rigaud, P.; Armand, M. B.; Deroo, D. *J. Electrochem. Soc.* **1985**, *132*, 1333.

S0020-1669(97)00611-3 CCC: $14.00

complex melts and how they depend on temperature. The dependency of viscosity, differential scanning calorimetry, electronic spectroscopy, and dilute solution voltammetry on the number of polyether tails is also examined.

The undiluted $[Ru(bpy)_N(bpy(CO_2MePEG\text{-}350)_2)_{3-N}](ClO_4)_2$ melts are highly viscous, and their ionic conductivities and the physical self-diffusion coefficients (D_{phys}) of the metal complexes can be expected to be quite small. During oxidative voltammetry of the undiluted melts, mixed-valent layers of Ru(III/II) complexes form around the microelectrode. The combination of small D_{phys} values and the generally large self-exchange rate constants, k_{ex}, of the Ru(III/II) redox couples leads to a transport process in which coupling between physical diffusion and electron hopping occurs, producing a net or apparent diffusivity D_{app} as given by the Dahms−Ruff relation (in its corrected[6] form)

$$D_{app} = D_{phys} + \frac{k_{ex}\delta^2 C}{6} \qquad (1)$$

where C and δ are the concentration and average center-to-center distance between the complexes in the melt, respectively. The right-hand term in eq 1 is sometimes called the electron diffusion coefficient, D_e. This equation, first applied to redox polymers by Buttry and Anson,[7] has since been widely applied to charge transport situations in the mixed-valent layers formed at electrode surfaces during voltammetry.[6] In the present context, it provides an avenue for evaluation of the electron self-exchange rate constants of the Ru(III/II) and Ru(II/I) couples in the semisolid Ru complex molten salts.

"Supporting electrolytes", which are added to dilute solutions of redox species in voltammetrically studied fluid solvents to enhance ionic conductivity and to mitigate ionic "migration" effects, are not used in the present Ru complexes and in analogous Co and Fe complex melts, since the intrinsic ionic conductivities of the melts are sufficient for microelectrode voltammetry. The ionic conductivities of the pure Ru melts (like the Co and Fe analogs)[1g] indicate that ClO_4^- is more mobile than either the metal complex ion or the exchanged electrons. Thus, although no $LiClO_4$ electrolyte was added, there is no significant ionic migration effect or consequence in the use of eq 1. It is pertinent to note that dissolution of $LiClO_4$ in the metal complex melts produces substantial changes: depression of transport parameters, elevation of viscosity, and even depression of the ionic conductivity. A detailed study of these effects will be shortly described for the Co complex melts.[1j]

Results and Discussion

Solubilities and Synthesis. Solubilities over a range of solvents and lack of crystallinity of the tailed Ru complexes make high-yield synthetic pathways desirable to minimize difficulties in purification (see Experimental Section). Attaching short polyether chains confers intermediates and products with the wide-ranging solubilities typical of polyethers, increasingly so as the molecular proportion of the polyether tail increases, and more so for neutral than for charged species. As a result, the tailed ruthenium complexes are soluble in solvents as polar as water and propylene carbonate (PC) and as nonpolar as CCl_4 and benzene. They are insoluble in poly(propylene oxide) and poly(siloxanes), Et_2O, toluene, and hexanes and slightly soluble in 2-propanol and ethyl acetate. Unattached polyether chains have similar solubilities and adsorption chromatographic retention times. While neutral tailed Ru complexes and tailless impurities are separable by silica gel chromatography, the tailed cationic Ru complexes adsorb strongly and are difficult to elute. Attempts at purification with gel permeation and ion exchange chromatographies were unsuccessful.

Table 1. Physical Properties of the Tailed Ru Complex Melts

species	MW	ρ, g/cm^3	concn, M	molec vol, Å^3	T_G, K	ΔC_P, J/(g·deg)	log(η (cP)) at 25 °C
2-tail	1520	1.42	0.936	1775	271	0.4	6.94
4-tail	2272	1.36	0.597	2783	250	0.6	6.02
6-tail	3024	1.30	0.429	3871	224	0.7	4.64
MePEG350	350	1.09		531			

A "one-pot" reaction in PC at moderate temperatures affords the 2- and 4-tail complexes in high yield (see Experimental Section). The PC solvent stabilizes the intermediates formed in the Ag^+ dechlorinations of $[Ru(bpy)_2Cl_2]$ and $[Ru(bpy(CO_2MePEG350)_2)_2Cl_2]$, allowing them to react with $bpy(CO_2MePEG350)_2$ and bpy, respectively.[8] A DMSO−ruthenium complex was used in the preparation of the 6-tail complex. The ethyl ester analogs of the three Ru complexes were also prepared as an aid in confirming structures and in assaying the purity of the tailed Ru complexes. The ester analogs are readily purified by recrystallization and have dilute solution voltammetry and electronic spectra similar to those of the tailed complexes.

Densities. Physical properties of the Ru complex melts are summarized in Table 1. Density (ρ) measurements provide molar concentrations (Table 1) and metal−metal spacings (δ) and are used to monitor volume contraction effects. In conventional polyether polymer electrolytes, cohesive forces between the polyether solvent and electrolyte (e.g., $LiClO_4$) can effect a volume contraction, thereby elevating the electrolyte concentration above that calculated by assuming molar volume additivity of the electrolyte and polyether.[9] In our case, the "electrolyte" is the core $[Ru(bpy)_3]^{2+}$ ion and its ClO_4^- counterions, and the "solvent" is the attached MePEG350 polyether chains. A plot of the molecular volumes in Table 1 against the number of attached MePEG350 chains is linear with a 524 Å^3/chain slope that, within experimental uncertainty, equals the 531 Å^3/molecule volume determined for pure MePEG350. The large volume contraction effects seen[9] in $LiClO_4$/polyether solutions seem to be precluded by the rigidity of the metal complex core in the present case. The 714 Å^3 intercept of the plot is close to the 775 Å^3/molecule volume of $[Ru(bpy)_3](ClO_4)_2$, obtained from crystal density measurements.[10]

Voltammetry of Dilute Solutions of the Complexes. Dilute acetonitrile solutions of the tailed Ru complexes exhibit well-defined, generally reversible, cyclic voltammetry (Figure 1). The

(5) (a) Nishihara, H.; Dalton, F.; Murray, R. W. *Anal. Chem.* **1991**, *63*, 2955. (b) Wooster, T. T.; Longmire, M. L.; Watanabe, M.; Murray, R. W. *J. Phys. Chem.* **1991**, *95*, 5315. (c) Wooster, T. T.; Watanabe, M.; Murray, R. W. *J. Phys. Chem.* **1992**, *96*, 5886. (d) Zhang, H.; Murray, R. W. *J. Am. Chem. Soc.* **1993**, *115*, 2335. (e) Pyati, R.; Murray, R. W. *J. Am. Chem. Soc.* **1996**, *118*, 1743. (f) Watanabe, M.; Longmire, M. L.; Murray, R. W. *J. Phys. Chem.* **1990**, *94*, 2614. (g) Terrill, R. H.; Sheenan, P. E.; Long, V. C.; Washburn, S.; Murray, R. W. *J. Phys. Chem.* **1994**, *98*, 5127.

(6) (a) Majda, M. In *Molecular Design of Electrode Surfaces*; Murray, R. W., Ed.; Wiley: New York, 1992. (b) Botar, L.; Ruff, I. *Chem. Phys. Lett.* **1986**, *126*, 348.

(7) Buttry, D. A.; Anson, F. C. *J. Electroanal. Chem.* **1991**, *130*, 333.

(8) Dichloromethane and dichloroethane are too nonpolar for the dechlorination reaction to proceed, and alcohols compete with the subsequent bipyridine ligation.

(9) (a) Moacanin, J.; Cuddihy, E. F. *J. Polym. Sci.: Part C* **1966**, *14*, 313. (b) Le Nest, J.-F.; Gandini, A.; Cheradame, H.; Cohen-Addad, J.-P. *Macromolecules* **1988**, *21*, 117.

(10) The molecular volume of $[Ru(bpy)_3](ClO_4)_2$ was derived from the density (1.70 g/cm^3) obtained by flotation in an aqueous $NaClO_4$−NaI solution.

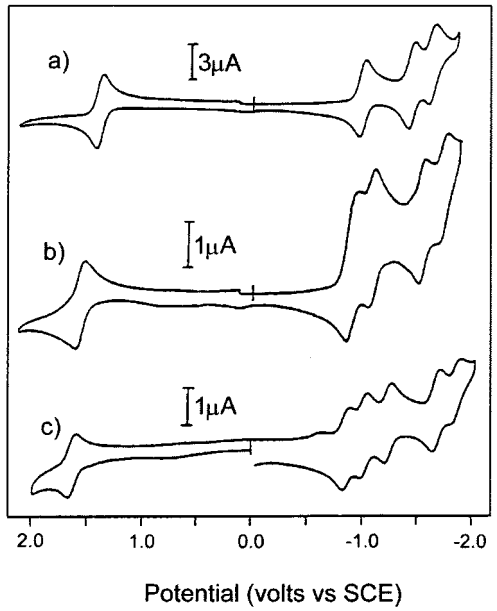

Figure 1. Cyclic voltammetry (200 mV/s) of $[Ru(bpy)_N(bpy(CO_2MePEG350)_2)_{3-N}](ClO_4)_2$ complexes in 0.1 M Bu_4NPF_6/acetonitrile at a Pt disk electrode (0.47 mm diameter): (a) 2-tail (6.1 mM), (b) 4-tail (2.5 mM), (c) 6-tail (3.2 mM) species. See Table 2.

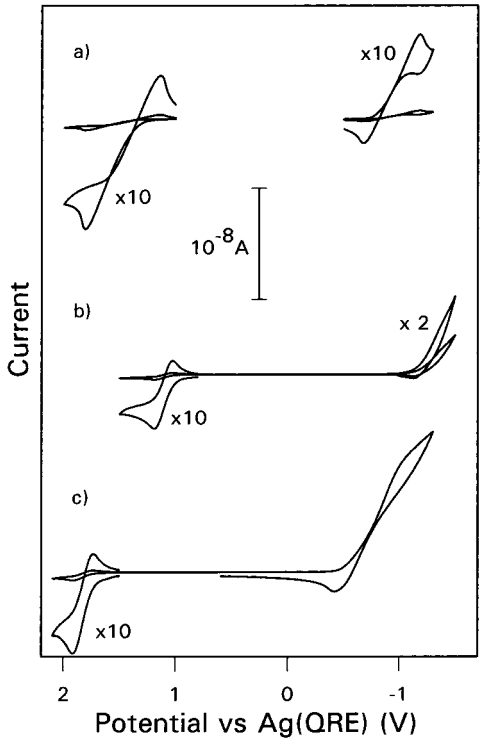

Figure 2. Cyclic voltammetry of undiluted $[Ru(bpy)_N(bpy(CO_2MePEG350)_2)_{3-N}](ClO_4)_2$ complex melts at a Pt microelectrode (radius 6.26 μm); temperature = 50 °C: (a) 2-tail, 5 mV/s; (b) 4-tail, 10 mV/s; (c) 6-tail, 50 mV/s.

observed formal potentials (see Supporting Information, Table S-1) for the Ru(III/II) waves roughly agree with those predicted using the ligand additivity principle introduced by Lever,[11] given that $E_L(bpy) = 0.259$ V and $E_L(bpy(CO_2MePEG350)_2) = 0.312$ V *vs* NHE. From a mechanistic viewpoint, consistency with the ligand additivity prediction indicates that each $bpy(CO_2MePEG350)_2$ ligand removes a constant amount of charge density from the ruthenium, linearly lowering the ruthenium potential.

The multiple voltammetric reduction waves are clustered in two groups separated by a gap, all of which can be assigned to reductions of the bipyridine rings.[12] In the 2-tail complex voltammogram (Figure 1a), owing to its electron-withdrawing ester linkages, reduction of the $bpy(CO_2MePEG350)_2$ ring occurs at the more positive potential. The 4-tail and 6-tail complexes exhibit two and three $bpy(CO_2MePEG350)_2$ ring reduction steps, respectively, at similarly positive potentials (Figure 1b,c). The more negative reductions in each case are attributed to those of the *tailless* bipyridines and to the second electron reductions of some of the tailed bipyridines. In the case of the 6-tail complex, for example, there are no tailless bipyridines; hence, the two waves appearing at more negative potentials must reflect addition of a second electron to two of the $bpy(CO_2MePEG350)_2$ ligands.

Electrochemistry in Undiluted Ru Complex Molten Salts. The tailed Ru complexes are concentrated molten salts and as such are unique forms of the ruthenium tris(bipyridine) complex. Films of ruthenium polypyridine complexes have been described before[13] on electrodes as electropolymerized metal complexes and with ruthenium tris(bipyridine) as counterion in Nafion films. While these earlier, semisolid forms of the Ru complex provide insights for interpreting the present data, the $[Ru(bpy)_3]^{2+}$ centers in the melts differ in the capacity for systematic structural variations (i.e., the quantity of attached polyether "solvent") and in that they and the "solvent" are codiffusants.

Microelectrode cyclic voltammograms of the three Ru melts are shown in Figure 2. Ionic conductivities of the Ru complex melts are modest (10^{-6}–10^{-8} Ω^{-1} cm^{-1} depending on the number of tails), and a combination of microelectrodes and slow potential sweeps is needed to mitigate the otherwise overwhelming uncompensated resistances. The voltammetry is well formed although there are obvious resistance distortions.[14] Only a single reduction step could be accessed. The voltammetry is least satisfactory for the 4-tail Ru(II/I) reduction wave. Values of apparent diffusion coefficients (D_{app}) for the Ru(III/II) oxidation and Ru(II/I) reduction reactions (Table 2) were obtained by matching the experimental voltammograms to digital simulations (see Experimental Section). For the room-temperature Ru(III/II) couple, D_{app} is largest for the 2-tail complex but there seems to be no systematic trend with the number of tails. For the Ru(II/I) couple, there is a clear trend; D_{app} increases 80-fold with the increased number of tails.

(11) (a) Lever, A. B. P. *Inorg. Chem.* **1990**, *29*, 1270. (b) The metal redox potential, $E(M^{n+1/n})$, of a coordination complex can be predicted by summing the influence each ligand has on it:

$$E(M^{n+1/n}) = S_M[\Sigma a_i E_L(L_i)] + I_M$$

A particular ligand, L_i, contributes an amount $E_L(L_i)$ multiplied by the number of coordination sites it occupies, a_i, and S_M and I_M are contants specific to the metal couple (e.g., $Ru^{3+/2+}$, $Ru^{4+/3+}$, $Cr^{3+/2+}$, etc.). $E_L(L_i)$, S_M, and I_M values are listed in ref 11a. Using the equation, $E_L(bpy(CO_2MePEG350)_2)$ was determined using the $E(Ru^{3+/2+})$ value of the 6-tail complex and $S_M(Ru^{3+/2+}) = 1$ and $I_M(Ru^{3+/2+}) = 0$.

(12) Meyer, T. J. *Acc. Chem. Res.* **1979**, *11*, 94 (and references therein).

(13) (a) Denisevich, P.; Abruna, H. D.; Leidner, C. R.; Meyer, T. J.; Murray, R. W. *Inorg. Chem.* **1982**, *21*, 2153. (b) Martin, C. R.; Rubinstein, I.; Bard, A. J. *J. Am. Chem. Soc.* **1982**, *104*, 4817.

(14) The 2-tail melt cyclic voltammogram exhibits a reproducible crossover of the positive and negative current−potential traces (Figure 2a), which is more prominent at lower temperatures. A 25 °C ac impedance spectrum taken at a nonfaradic potential gives a melt resistivity of 9 × 10^7 Ω cm, which corresponds to $R_{unc} = 4 \times 10^{10}$ Ω at the microelectrode. However a computer simulation of a reversible voltammogram (matching peak positions and currents, incorporating the value for D_{app}) gives a much smaller value, $R_{unc} = 3 \times 10^9$ Ω, at the microelectrode. The difference suggests that the crossover anomaly arises from a decrease in R_{unc} as the more conductive mixed-valent melt forms around the electrode during the negative potential scan.

Table 2. Transport Measurements in Undiluted, Molten Salt Tailed Ru Complexes

		Ru(III/II)[a]				Ru(II/I)[a]			
Ru complex	δ,[b] Å	D_{app} (25 °C), $cm^2\ s^{-1}$	k_{ex} (25 °C), $M^{-1}\ s^{-1}$	E_A,[c] kJ/mol	$k_{ex}°$,[c] $M^{-1}\ s^{-1}$	D_{app} (25 °C), $cm^2\ s^{-1}$	k_{ex} (25 °C), $M^{-1}\ s^{-1}$	E_A,[d] kJ/mol	$k_{ex}°$,[d] $M^{-1}\ s^{-1}$
2-tail	12.1	1.1×10^{-9}	5×10^5	26 ± 2	2×10^{10}	5×10^{-10}	2×10^5	45 ± 1	1×10^{13}
4-tail	14.1	8×10^{-11}	4×10^4	36 ± 4	1×10^{11}	9×10^{-9}	4×10^6	(16 ± 3)	(3×10^9)
6-tail	15.7	2.8×10^{-10}	1.6×10^5	33 ± 1	1×10^{11}	4×10^{-8}	3×10^7	22 ± 1	2×10^{11}

[a] Results for Ru(III/II) and Ru(II/I) were obtained in separate experiments. [b] Calculated from melt density and molecular weight (Table 1), using $\delta = (10^{24}(MW)/\rho N_A)^{1/3}$. [c] From slope and intercept of activation plots as in Figure 3a; linear regression coefficients are 0.986, 0.980, 0.998 for 2-, 4-, 6-tail complexes. Uncertainties of the intercepts are roughly a factor of ±10. [d] From slope and intercept of activation plots as in Figure 3b; linear regression coefficients are 0.998, 0.90, 0.987 for 2-, 4-, 6-tail complexes. Uncertainties of the intercepts are roughly a factor of ±10.

Table 3. Ionic Conductivity Results (Figure 2)

Ru complex	log σ_{ion} (25 °C)	$E_{A,ion}$, kJ/mol	ln σ_0[a]	T_0,[a] K
2-tail	−7.95	26	7.81	163
4-tail	−6.82	14	1.59	179
6-tail	−6.17	8.4	−2.04	190

[a] From VTF fit, Figure 3.

Consider the D_{app} results (Table 2) for the Ru(III/II) couple in the light of eq 1. An estimate of the physical self-diffusivity, D_{phys}, of the ruthenium sites in the melt is required in order to assess the contribution of electron self-exchanges to D_{app}. For this purpose, the 6-tailed Co complex melt, $[Co(bpy(CO_2\text{-}MePEG350)_2)_3](ClO_4)_2$, is a convenient surrogate. First, its very small[15] electron self-exchange rate constant (2 $M^{-1}\ s^{-1}$) ensures that electron hopping does not contribute to transport in the Co(III/II) reaction of the complex (e.g., D_e in eq 1 is 4×10^{-15} cm^2/s, and probably much less,[1a,f,g] so the measured diffusivity of $[Co(bpy(CO_2MePEG350)_2)_3]^{2+}$ (1.3×10^{-11} cm^2/s) can be taken as D_{phys} for the complex in its room-temperature melt). Second, the $[Co(bpy(CO_2MePEG350)_2)_3]^{2+}$ complex is isostructural with the 6-tail $[Ru(bpy(CO_2MePEG350)_2)_3]^{2+}$ complex; thus, their physical diffusivities should be similar. In support of this analogy (which has also been used in the transport analysis of an identically 6-tailed Fe complex[1f,g]), the ionic conductivities 6.4×10^{-7} [1g] and 6.8×10^{-7} $\Omega^{-1}\ cm^{-1}$ (Table 3) of the Co and Ru melts, respectively, are identical, and their viscosities, 2×10^4 [1g] and 4×10^4 cP (Table 1), nearly so.

Accordingly, $D_{phys} = 1.3 \times 10^{-11}$ cm^2/s is taken for $[Ru(bpy(CO_2MePEG350)_2)_3]^{2+}$ in the 6-tail Ru complex melt and, in comparison to the $D_{app} = 2.8 \times 10^{-10}$ cm^2/s measured for the Ru(III/II) reaction (Table 2), contributes an insignificant 5% to the D_{app} value. While we have no analogous surrogate diffusion models for the 4-tail and 2-tail Ru complexes, their 24- and 200-fold larger viscosities, respectively (Table 1), make it highly likely that their physical diffusivities are even smaller than that of the 6-tail complex, and their D_{phys} values were assumed to be negligible in relation to the D_{app} results (which also decrease, but by less than the factor in viscosity). On the basis of the preceding, electron self-exchange rate constants were calculated from eq 1 for the three Ru(III/II) couples. Table 2 shows that the k_{ex} rate constants are all on the order of 10^5 $M^{-1}\ s^{-1}$.

For the Ru(II/I) couple, D_{app} for the 2-tail melt is not very different from that of the Ru(III/II) couple, but for the 4- and 6-tail melts it is substantially larger. The k_{ex} values for the Ru(II/I) couple were calculated in the same way as those of the Ru(III/II) couple (D_{phys} negligible), giving the results in Table 2.

The temperature dependencies of D_{app} for the Ru(III/II) and Ru(II/I) reactions were also measured; conversion to k_{ex} values and neglecting D_{phys} as above gave linear activation plots (Supporting Information, Figure S-I) from which activation barriers, E_A, and $1/T = 0$ intercepts, $k_{ex}°$, were extracted (Table 2). The activation results for the 4-tail complex's Ru(II/I) reaction, shown parenthetically, are of low reliability owing to the abbreviated temperature range and relatively poor voltammetry (Figure 2b).

Consideration of Transport Results in Undiluted Ru Complex Melts. The results in Table 2 show that the 25 °C rate constants (k_{ex}) for the Ru(III/II) electron self-exchange reaction lie within an order of magnitude of one another, as do the activation plot ($k_{ex}°$) intercepts. The Ru(III/II) results exhibit no systematic trends and for the present discussion are regarded as kinetically similar.

It is useful to consider the Ru(III/II) data (Table 2) in the light of recent work on analogous, undiluted 6-tail Co and Fe complex melts,[1g] where rate and activation parameters for the Co(II/I) and Fe(III/II) reactions were measured as a function of polyether tail length. The activation barrier energies ranged from 25 to 36 kJ/mol, and the activation plot intercepts ($k_{ex}°$) ranged from 10^{10} to 10^{12} $M^{-1}\ s^{-1}$. Significantly, while physical diffusivities (D_{phys} was obtained from the Co(III/II) couple) were strongly depressed by shorter polyether tails, the Co(II/I) and Fe(III/II) room-temperature electron transfer rate constants were *insensitive to tail length*.

The interpretation[1g] given the Co(II/I) and Fe(III/II) results was, briefly, as follows: (a) The polyether-tailed metal complexes are regarded as "hard" (metal bipyridine) cores covered with "soft", solvent-like (polyether) shells that, through fluctuating chain segment rearrangements, are highly deformable. Physical diffusion of the bulky complexes past one another in the undiluted melts is facilitated by thicker, deformable polyether shells (longer or more numerous chains). (b) The insensitivity of k_{ex} values to changes in the average center-to-center distances between metal complexes (produced by variation of the average polyether shell thickness) strongly implies that the metal complex cores vibrate within their fluctuating polyether shells at a frequency greater than that of the electron transfers, and to reasonably close encounter distances. Otherwise, the distance changes would cause the rate constants to decrease with longer polyether chains. This and the large magnitudes of $k_{ex}°$ show that the Co(II/I) and Fe(III/II) electron transfers are adiabatic or nearly so. (c) The analysis is entirely consistent with recent effects seen[1f] in percolative electron transport in an Fe complex melt, suggesting that values of D_{phys} do not adequately measure the dynamics of *short-range (molecular dimension) fluctuations of the electron transfer sites, which can be faster*. (d) The Co(II/I) and Fe(III/II) electron transfer activation barriers are much larger than that expected for an "outer-sphere reorganizational barrier" of the metal complex core in an oligoether solvent.

We propose a similar interpretation of the Ru(III/II) electron transfer data (Table 2). The (rough) insensitivity of the room-

(15) Baker, B. R.; Basolo, F.; Neumann, H. M. *J. Phys. Chem.* **1959**, *63*, 371.

temperature Ru(III/II) k_{ex} values to the number of polyether chains suggests a rapid fluctuation of the metal complex cores within their polyether shells and electron transfers at relatively close distances. In terms of electron-hopping frequencies, for the 6-tail complex, for example, the electron-hopping frequency ($k_{ex}C$) is *ca.* 7×10^4 s^{-1} and the fluctuation of cores within the polyether shells is inferred to occur at much larger frequencies. The diffusional jump frequencies (D_{phys}/δ^2, jumps leading to physical transport across multiple complex dimensions) are in contrast much slower: *ca.* 500 s^{-1} for the 6-tail complex. The thin (average) polyether shells of the 2-tail and 4-tail complexes should lead to slowed physical diffusivities relative to that of the 6-tail complex, an argument (connected to our neglect of D_{phys} in relation to their D_{app} values) that is consistent with the observed higher viscosities of the 2-tail and 4-tail metal complex melts.

In the expression for a bimolecular electron transfer reaction[16]

$$k_{ex} = K_A \kappa \nu \exp\left(-\frac{\Delta G^*}{k_B T}\right) \quad (2)$$

K_A is the donor−acceptor precursor complex formation constant, κ and ν are the electronic and frequency factors, respectively, and ΔG^* is the activation free energy for electron transfer. K_A for the $[Ru(bpy)_N(bpy(CO_2MePEG\text{-}350)_2)_{3-N}](ClO_4)_2$ melts is nearly unity[17a] (1.05 M^{-1}), and the (Table 2) activation barriers E_A can be equated[17b] with ΔG^* since reaction entropy[17c] and entropy of activation (ΔS^*)[17d] are zero. The activation plot intercepts k_{ex}° (Table 2) can thus be equated with $K_A\kappa\nu$ of eq 2, and given that $K_A \approx 1$ M^{-1}, the k_{ex}° results show that $\kappa\nu$ is *ca.* $10^{10}-10^{11}$ s^{-1} for the Ru(III/II) melt electron transfers. Like the Fe(III/II) and Co(II/I) results in analogous metal complex melts, the Ru(III/II) electron transfer reaction is nearly adiabatic.

Also like the Fe(III/II) and Co(II/I) results,[1g] the room-temperature Ru(III/II) k_{ex} constants in Table 2 are much smaller than that known for the Ru(III/II) reaction in the analogous $[Ru(bpy)_3]^{2+}$ complex dissolved in fluid solution (10^7 M^{-1} s^{-1}).[18] Such differences are nearly always seen when mixed-valent polymer-phase self-exchanges are compared with monomer fluid solution rates.[1fg,3a,19] The results for the polyether-tailed metal complex melts suggest that the most general reason for the slowed kinetics is an increased activation barrier energy for the electron transfers. The "outer-sphere" reorganizational barrier energy for the Ru(III/II) melt electron transfer can be estimated[20] as 8−10 kJ/mol by considering the metal complex core to be embedded in an ether solvent shell (the polyether tails) and using the classical Marcus[21] dielectric continuum model. These values are 2−3-fold smaller than experimental E_A results (Table 2) for the Ru(III/II) barriers. Given that the nuclear coordinates in the related unsubstituted complexes, $[Ru(bpy)_3]^{2+}$ and $[Ru(bpy)_3]^{3+}$, are the same,[16d] an "inner-sphere reorganizational energy barrier" of the classical kind[21] is not expected. The experimental activation barrier energies thus appear to contain an additional, unusual, term, about which we have speculated[1g] as (i) a peculiar "inner-sphere-like" barrier term associated with the linkage between the bpy ligand and its "ether solvent shell" or (ii) a barrier associated with reorientation dynamics of the ether dipoles in the "solvent shell" (i.e., solvent dynamics).

A previous discussion[19b] regarding electron transfer rates in electropolymerized Os bipyridine films pointed out that rates were slowed in the presence of increased cross-linking in the polymer and hypothesized that "the polymer lattice can, under rigidified circumstances, impose an inner-sphere-like barrier". The electron transfer kinetics of the metal complex melts are consistent with this earlier comment, but the melts give us opportunity to sharpen the analysis by providing environments around the reacting metal complexes (the polyether shell) that can be manipulated (length and number of polyether chains) and whose dielectric properties can be tested against conventional theory. The systematic structural variations possible with the polyether-tailed metal complex melts are not readily available in the polymerized materials. We believe that the melt-forming capacity of attached polyether chains will be a useful anvil against which to further hammer out a more detailed understanding of the microscopic details of solid and semisolid state electron transfer chemistry.

Finally, we turn to the Ru(II/I) electron self-exchange rate constants (Table 2), which increase substantially with the number of polyether tails. This trend is somewhat difficult to rationalize. The Ru(II/I) reaction is unique among the others (i.e., Fe(III/II), Ru(III/II), and Co(II/I)) both in its kinetic sensitivity to the variation of polyether tail proportion and in being a ligand-centered reaction as opposed to a metal-centered reaction. That is, the self-exchange reaction is one between Ru-coordinated bpy and $bpy^{\bullet-}$ rings (and more specifically, given the spacing between ring LUMO revealed by the voltammetry in Figure 1, between the tail-bearing ligands). From previous work[22] demonstrating that electrons can exchange very rapidly (10^{10} s^{-1}) between (alike) bpy rings in the $[Ru(bpy)_3]^{+}$ complex, it can be expected that, in the Ru(II/I) reaction, electrons can enter and exit the 6-tail [Ru(bpy(CO_2Me-

(16) (a) Marcus, R. A.; Sutin, N. *Biochim. Biophys. Acta.* **1985**, *811*, 265. (b) Marcus, R. A.; Siddarth, P. In *Photoprocesses in Transition Metal Complexes, Biosystems, and Other Molecules*; Kochanski, E., Ed.; Kluwer Dordrecht, The Netherlands, 1992. (c) Sutin, N. *Acc. Chem. Res.* **1982**, *15*, 275. (d) Sutin, N. *Prog. Inorg. Chem.* **1983**, *30*, 441. (e) Newton, M. D.; Sutin, N. *Annu. Rev. Phys. Chem.* **1984**, *35*, 437.

(17) (a) K_A was calculated from[16d]

$$K_A = \frac{4\pi N_A \bar{r}^2 \delta\bar{r}}{10^3}$$

A work term is not included since the reacting complexes are essentially already in contact. The center-to-center distance, *r*, is taken as that for the E_3M tailed complex, 13.2 Å, and δr is taken[16d] as 0.8 Å. (b) Neglecting $\Delta S_\lambda^\ddagger$, reorganization entropy.[16e] (c) Given that the reaction measured is an electron self-exchange process.[16b,e] (d) There is no work term.[17a]

(18) Chan, M.-S.; Wahl, A. C. *J. Phys. Chem.* **1978**, *82*, 2542.

(19) (a) Studies of electropolymerized films of Os(III/II) vinylpyridines[19b] and vinylbipyridines[19c] give activation barriers near 35 kJ/mol and intercepts near 10^{11} M^{-1} s^{-1}. (b) Surridge, N. A.; Zvanut, M. E.; Keene, F. R.; Sosnoff, C. S.; Silver, M.; Murray, R. W. *J. Phys. Chem.* **1992**, *96*, 962. (c) Jernigan, J. C.; Surridge, N. A.; Zvanut, M. E.; Silver, M.; Murray, R. W. *J. Phys. Chem.* **1989**, *93*, 4620.

(20) (a) The "outer-sphere" reorganization barrier was estimated using

$$\Delta G^*_{out} = \frac{N(\Delta e)^2}{16\pi\epsilon_0}\left(\frac{1}{2a_1}+\frac{1}{2a_2}-\frac{1}{r}\right)\left(\frac{1}{D_{op}}-\frac{1}{D_s}\right)$$

where a_1 and a_2 are the reactant radii and r is their center−center distance, Δe is the charge transferred in the reaction, ϵ_0 is the permittivity of a vacuum, N is Avogadro's number, and D_{op} and D_s are the solvent optical and static dielectric constants, respectively. Assuming $r = 2a_1 = 2a_2 = \delta$ (Table 2) and using[5e] $D_{op} = 2.128$ and $D_s = 9.16$ for the polyether MePEG400, ΔG^*_{out} is, for the 6-tail complex, 8.0 kJ/mol; for the 4-tail complex, 8.9 kJ/mol; for the 2-tail complex, 10.3 kJ/mol; and for the tailless $[Ru(bpy)_3]^{2+}$ complex (r = 9.09 Å, estimated from crystallographic density), 13.9 kJ/mol. Taking[20b] r = 13.6 Å for tailless $[Ru(bpy)_3]^{2+}$ gives $\Delta G^*_{out} = 9.2$ kJ/mol. Outer-sphere barrier energies as large as those in Table 2 for Ru(III/II) cannot be obtained from the above equation by any physically reasonable choices of distances or dielectric properties. (b) Brunschwig, B. S.; Creutz, C.; Macartney, D. H.; Sham, T.-K.; Sutin, N. *Faraday Discuss. Chem. Soc.* **1982**, *74*, 113.

(21) (a) Marcus, R. A.; Sutin, N. *Biochim. Biophys. Acta* **1985**, *811*, 265. (b) Marcus, R. A. *J. Chem. Phys.* **1965**, *43*, 679.

(22) Motten, A. G.; Hanck, K.; DeArmond, M. K. *Chem. Phys. Lett.* **1981**, *79*, 541.

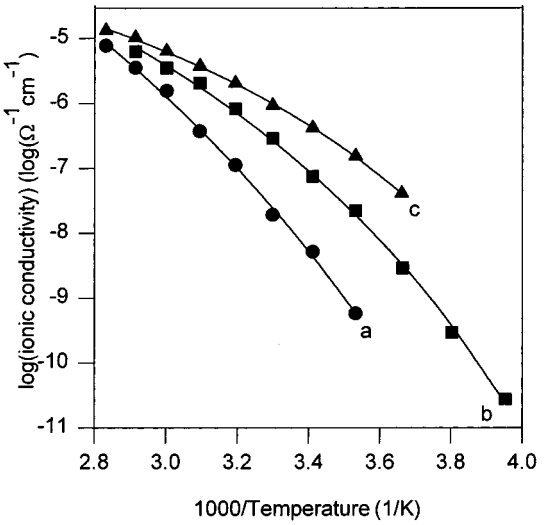

Figure 3. Activation plots of ionic conductivity of the $[Ru(bpy)_N(bpy(CO_2MePEG350)_2)_{3-N}](ClO_4)_2$ complexes: (a) 2-tail, (b) 4-tail, (c) 6-tail species. The lines joining the points are VTF fits. See Table 3 for parameters.

$PEG350)_2)_3]^{2+}$ and $[Ru(bpy(CO_2MePEG350)_2)_3]^+$ complexes, respectively, from any direction. This would not be so for the 2-tail complex. Consider a hypothesis in which electron exchange between the 2-tail complexes $[Ru(bpy)_2(bpy(CO_2MePEG\text{-}350)_2)]^{2+}$ and $[Ru(bpy)_2(bpy(CO_2MePEG\text{-}350)_2)]^+$ (where intracomplex ring exchange reactions should be comparatively slow) would require either a rotation of the complexes so as to juxtapose the tail-bearing bpy rings or, if the rotational correlation time is sufficiently long, a longer distance (and thus slower) bpy/bpy$^{\bullet-}$ electron transfer. Calculation using the Stokes−Einstein equation [$\tau_C = (4\pi\eta r^3/3k_BT)^{-1}$] of the rotational frequency of the 2-tail complex produces a result, 500 s^{-1}, that in fact is much slower than the Ru(II/I) electron-hopping frequency for that complex ($k_{ex}C \approx 2 \times 10^5$ s^{-1}). Use of the Stokes−Einstein equation in these circumstances is probably approximate; this interesting hypothesis of rotation-frequency-dominated electron transfer rates could conceivably be explored by more direct measures of rotational dynamics in the melts.

Viscosity and Differential Scanning Calorimetry. The viscosities of the Ru complex melts are large and increase by orders of magnitude with decreasing numbers of attached MePEG350 chains (Table 1). The viscosities range from 4×10^4 cP for the 6-tail complex to almost 10^7 cP for the 2-tail complex. Analogous changes occur in the tailed Co bipyridine complexes where viscosity increases as the length of the attached MePEG chains is decreased.[1g] These changes are consistent with the above-cited importance of polyether chain deformation to macroscopic physical displacements in the melts.

The Ru complex melts exhibit a glassing transition by differential scanning calorimetry, with no evidence of crystallinity. The glassing temperatures increase by 45 K as the number of attached MePEG350 chains decreases; a 20 K increase in T_G is associated with roughly a 10-fold viscosity increase (Table 1). The correlation between T_G, which reflects *microscopic* viscosity, and rheometric viscosity η, which reflects *macroscopic* viscosity, exists because the Ru complex melts are unentangled and un-cross-linked.[23] For unentangled polymers, microscopic and macroscopic viscosities parallel each other.[24] In polyether electrolyte solutions,[24,25] T_G and viscosity are also elevated by increasing electrolyte concentration. Also given in Table 1 are the heat capacity changes at T_G.

Ionic Conductivities. Room-temperature ionic conductivities of the Ru complex melts increase by *ca.* 70-fold from the 2-tail to the 6-tail complex (Table 3), even though the formal ionic concentration in the 6-tail complex is 2-fold smaller. The changes in ionic conductivity are primarily governed by changes in viscosity. A similar conclusion has been reached regarding polyethers with anionic termini.[26]

Arrhenius plots of the ionic conductivities (Figure 3) for the Ru complex melts are curved as typical for physical processes strongly coupled to the segmental motions of polymer chains. The plots were analyzed using the Vogel−Tamman−Fulcher (VTF)[27] equation, which written for ionic conductivities, is[28]

$$\sigma = \sigma_0 T^{-1/2} \exp\left[\frac{E_{A,ion}}{R(T - T_0)}\right] \qquad (3)$$

where σ_0 is related to the concentration of charge carriers, $E_{A,ion}$ is a pseudoactivation energy for chain segmental motion coupled to ion motion, R is the gas constant, and T_0 is the temperature at which configurational entropy or free volume drops to zero, i.e., where the relaxation times of the polymer chains become infinite. Results for VTF fits are shown in Table 3. Commonly, alkali metal salt−polyether systems showing VTF behavior yield T_0 values that are 50 K lower than T_G.[27] This is not observed in the Ru complex melts; instead, T_0 rises while T_G falls. Perhaps this reflects the substantial structural difference that the Ru complex center introduces. Table 3 shows that $E_{A,ion}$ decreases with increasing number of tails, which is consistent with the accompanying decrease of viscosities since both ionic mobility and viscosity depend on segmental motion and its thermal activation.

The physical diffusivity of the $[Ru(bpy(CO_2MePEG350)_2)_3]^{2+}$ metal complex in its melt ($D_{phys} = 1.3 \times 10^{-11}$ cm^2/s) can be used along with the melt ionic conductivity and the Nernst−Einstein equation to calculate the diffusion coefficient of the ClO_4^- ion in the 6-tail complex melt.[1g] The result, $D_{ClO_4} = 1.4 \times 10^{-10}$ cm^2/s, shows that, as expected, ClO_4^- is the more mobile ion. These results give transference numbers for the Ru complex and its ClO_4^- counterion in the melt of $t_+ = 0.16$ and $t_- = 0.84$, respectively, showing that current flow is mainly carried by ClO_4^- and that D_{app} in the Ru melts is consequently not strongly affected by ionic migration. However, electron migration may affect the D_{app} values. Electron diffusion rates exceeding that of the counterion generate electric fields that cause electron migration, thereby enhancing the measured D_{app} and k_{ex} values for the Ru(III/II) reaction over their true ones. Such enhancement, which increases with the ratio D_{app}/D_{ClO_4}, can be evaluated for the 6-tail Ru complex melt according to Andrieux and Saveant.[29] Applying their theory gives corrections that are less than 10% of the measured D_{app} for the Ru(III/II) reaction, which is less than the probable experimental uncertainty. The electronic migration enhancement is, however, likely

(23) Sandahl, J.; Schantz, S.; Torrell, L. M.; Frech, R., *Solid State Ionics* **1988**, *28*−30, 958.
(24) McLin, M. G.; Angell, C. A. *J. Phys. Chem.*, **1991**, *95*, 9464.
(25) (a) Watanabe, M.; Ikeda, J.; Shinohara, I. *Polym. J.* **1983**, *15*, 177. (b) Watanabe, M.; Ogata, N. *Br. Polym. J.* **1988**, *20*, 181. (c) Eisenberg, A.; Ovans, K.; Yoon , H. N. *Adv. Chem. Ser.* **1980**, *187*, 267.
(26) Ito, K.; Ohno, H. *Solid State Ionics* **1995**, *79*, 300.
(27) (a) Vogel, H. *Phys. Z.* **1921**, *22*, 645. (b) Tamman, G.; Hesse, W. *Anorg. Allg. Chem.* **1926**, *156*, 245. (c) Fulcher, G. S. *J. Am. Ceram. Soc.* **1925**, *8*, 339.
(28) Ratner, M. A. In *Polymer Electrolyte Reviews−1*; MacCallum, J. R., Vincent, C. A., Eds.; Elsevier: New York, 1987. (b)Thatcher, J. H.; Thanapprapasr, K.; Nagae, S.-I.; Mai, S.-M.; Booth, C.; Owen, J. R. *J. Mater. Chem.* **1994**, *4*, 591.
(29) Andrieux, C. P.; Saveant, J. M. *J. Phys. Chem.* **1988**, *92*, 6761.

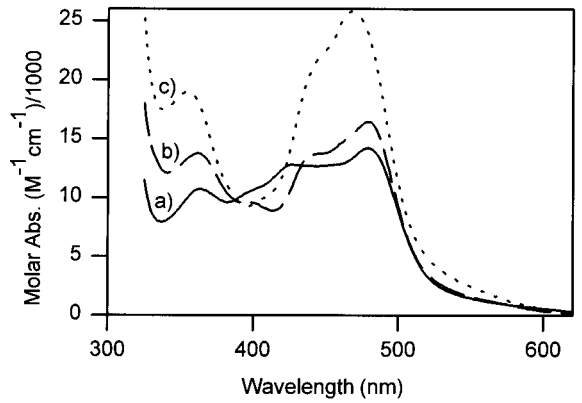

Figure 4. Electronic spectra of $[Ru(bpy)_N(bpy(CO_2MePEG350)_2)_{3-N}](ClO_4)_2$ solutions in acetonitrile: (a) 2-tail, (b) 4-tail, (c) 6-tail species. See Table S-II (Supporting Information).

to be more substantial in the 2-tail melt, since D_{ClO_4} must be smaller (according to ionic conductivity) and D_{app} larger (Table 2) than in the 6-tail melt. We lack the value of D_{phys} for the 2-tail melt to apply the appropriate correction to the Ru(III/II) rates; while it may be a severalfold factor (lowering D_{app}), it is nonetheless insignificant on the level of the preceding discussion of the kinetics.

Electronic Spectra. The dilute solution electronic spectra of the tailed and tailless ruthenium tris(bipyridine) complexes are nearly identical and exhibit three sets of charge transfer bands (Figure 4). The first set, with the most intense and lowest energy bands (around 468−479 nm), is assigned to a Ru → tailed-bpy $\pi^*(1)$ transition. Charge transfer transitions to the tailed bipyridine occur at lower energies than those to the tailless bipyridine due to the electron-withdrawing ester groups. Thus, $[Ru(bpy)_3]^{2+}$ has a band at 448 nm, whereas $[Ru(bpy(CO_2Et)_2)_3]^{2+}$ has one at 471 nm.[30] The second set of bands, around 400−450 nm, is assigned to the Ru → tailless-bpy $\pi^*(1)$ transition, and the third set of bands, at 354−364 nm, is due to a Ru → tailed-bpy $\pi^*(2)$ transition.[31]

In accord with the assignments, there is a systematic increase in the energy of all of the transitions as the number of tails/ester groups increases (data in Table SII). This results from a decrease in electron density at the metal, which is also reflected in the increase of Ru(III/II) potentials. Also notable is the systematic increase in the molar absorptivity of the Ru → tailed-bpy π^* transitions with increasing number of tails. The probability of having a Ru → tailed-bpy π^* transition increases with the number of tailed bipyridines present. The Ru → tailed-bpy π^* transitions have higher intensities than the Ru → bpy π^* transitions, as is evident from the difference in molar absorptivities of, for example, the Ru → $\pi^*(1)$ bands of $[Ru(bpy(CO_2Et)_2)_3]^{2+}$ (25 000 cm^{-1} M^{-1}) versus $[Ru(bpy)_3]^{2+}$ (14 600 M^{-1} cm^{-1}).[30a]

Experimental Section

Synthesis. Literature syntheses were followed for $[Ru(bpy)_2Cl_2]$ (bpy = 2,2′-bipyridine),[32] $bpy(CO_2MePEG350)_2$ (see Chart 1),[1g] 4,4′-bis(ethoxycarbonyl)-2,2′-bipyridine ($bpy(CO_2Et)_2$),[30a] and $[Ru(dmso)_4Cl_2]$ (dmso = dimethyl sulfoxide).[33] Distilled water was passed through a Barnstead Nanopure System Model 4754 purifier. Acetonitrile (Mallinckrodt AR) was freshly distilled over CaH_2 (Sigma) before use.

Proton NMR spectral data obtained on a Bruker AC-250 250 MHz or a Varian XL-400 400 MHz NMR spectrometer are reported versus TMS. Galbraith Laboratories (Knoxville, TN) performed the elemental analyses. Spectroscopic purities were determined by comparing the molar absorbances of the corresponding tailed and tailless ruthenium complexes at the Ru → bpy π^* band; *vide infra*.

Caution! Although no explosive difficulties have been encountered, the perchlorate salt melts should always be handled with care.

$[Ru(bpy(CO_2MePEG350)_2)_2Cl_2]$. A solution of $bpy(CO_2MePEG350)_2$ (0.75 g; 0.82 mmol) in 3 mL of dimethylfomamide (DMF) was added to a solution of $RuCl_3 \cdot 1-3H_2O$ (0.10 g; 0.41 mmol; Alfa Products) in 3 mL of DMF. The mixture was purged with argon and refluxed for 17 h. Flash evaporation of the resulting blue-green solution and drying *in vacuo* at 70 °C for 20 h gave a dark green oil with suspended white crystalline needles, which were removed by dissolving the oil in benzene (20 mL; Aldrich SureSeal) and filtering. The filtrate was flash-evaporated, and the resulting oil was chromatographed on silica (Davisil, grade 633), eluting with 90% acetone (Mallinckrodt AR)−H_2O. The first few fractions[34] from a main blue-green streak were collected and flash-evaporated to an oil. The oil was dried *in vacuo* at 70 °C for several days.

Anal. Calcd for $C_{84}H_{136}Cl_2N_4O_{36}Ru$; C, 51.74; H, 7.03; N, 2.87. Found: C, 53.10; H, 6.89; N, 3.31.

$[Ru(bpy(CO_2Et)_2)_2Cl_2]$. To a solution of $RuCl_3.2H_2O$ (0.50 g; 2.1 mmol) in 15 mL of DMF was added $bpy(CO_2Et)_2$ (1.2 g; 4.1 mmol). The mixture was purged with argon and refluxed for 10 h. Flash evaporation gave a dark green solid, which was washed with diethyl ether (Et_2O; Mallinckrodt AR) and redissolved in 50 mL of CH_2Cl_2 (Mallinckrodt AR). An impurity was removed by filtration, and the flash-evaporated crude product was chromatographed on silica, eluting with 20% acetone−CH_2Cl_2. The main blue-green fraction was collected and flash-evaporated to give a black product.

$[Ru(bpy)_2(bpy(CO_2MePEG350)_2)](ClO_4)_2$: 2-Tail Complex. To a 7 mL propylene carbonate (PC; Aldrich SureSeal) solution of $bpy(CO_2MePEG350)_2$ (0.30 g; 0.33 mmol) were added $[Ru(bpy)_2Cl_2]$ (0.16 g; 0.32 mmol) and $AgClO_4 \cdot H_2O$ (0.15 g; 0.65 mmol; Aldrich). The mixture was stirred for 15 h at 85 °C, giving a red-orange mixture containing AgCl, which was removed by centrifugation. The decantate was flash-evaporated to an oil at 85 °C under pump vacuum, precipitating more AgCl. The oil was dissolved in 5 mL of H_2O and centrifuged again. The decantate was extracted three times with benzene to remove unreacted ligand and PC. The aqueous layer was flash-evaporated, and the resulting red-brown oil was dried *in vacuo* at 70 °C for several days.

Spectroscopic purity: ϵ(tailed)/ϵ(tailless) = 1.04. Anal. Calcd for $C_{62}H_{84}Cl_2N_6O_{26}Ru$: C, 49.60; H, 5.64; N, 5.60. Found: C, 48.92; H, 5.69; N, 5.47. Proton NMR (as the nitrate salt) in $CDCl_3$ (7.24 ppm): δ 3.33 m (6H), 3.51 m (4H), 3.59−3.64 m (44H), 3.82 t (4H), 4.54 m (4H), 7.47 t (2H), 7.51 t (2H), 7.78 d (2H), 7.84 d (2H), 8.04 m (6H), 8.18 d (2H), 8.59 d (4H), 8.90 s (2H).

$[Ru(bpy)(bpy(CO_2MePEG350)_2)_2](ClO_4)_2$: 4-Tail Complex. Bipyridine (0.10 g; 0.63 mmol; Aldrich) and $AgClO_4 \cdot \sim 1H_2O$ (0.17 g; 0.85 mmol) were added to a solution of $[Ru(bpy(CO_2MePEG350)_2)_2Cl_2]$ (0.84 g; 0.42 mmol) in 10 mL of PC. The mixture was heated at 70 °C for 4 h. Upon cooling, 100 mL of anhydrous Et_2O was added, and the mixture was swirled for 10 min. The Et_2O−PC layer was decanted from the immiscible product, which was washed two more times with fresh Et_2O. To the resulting tacky red residue was added 15 mL of 90% ethanol (Aaper)−H_2O. The mixture was centrifuged to remove

(30) (a) Elliott, C. M.; Hershenhart, E. J. *J. Am. Chem. Soc.* **1982**, *104*, 7519. (b) Like that observed in $[Ru(bpy)_3]^{2+}$, the high-energy shoulder on the Ru → tailed-bpy π^* band arises from a splitting of the "t_{2g}" set of ruthenium d orbitals.

(31) This transition has an energy about 6500 cm^{-1} higher than the Ru → tailed-bpy $\pi^*(1)$ transition, approximately reflecting the energy gap between the $\pi^*(1)$ and $\pi^*(2)$ orbitals. The corresponding Ru → bpy $\pi^*(2)$ band from the $[Ru(bpy)_3]^{2+}$ spectrum should lie 6500 cm^{-1} higher than the Ru → bpy $\pi^*(1)$ band and is obscured by the intense ligand $\pi \rightarrow \pi^*$ band.

(32) Meyer, T. J.; Salmon, D. J.; Sullivan, B. P. *Inorg. Chem.* **1978**, *17*, 3334.

(33) Evans, I. P.; Spence, A.; Wilkinson, G. *J. Chem. Soc., Dalton Trans.* **1973**, 204.

(34) The compound streaks on the silica gel column. Collected fractions have similar spectra and solvatochromic properties, but earlier eluting fractions have lower R_f values in thin-layer chromatography and are more fluid when concentrated than those eluted later, indicating differences in composition. Probably, the later fractions have undergone some polyether tail cleavages.

AgCl. The decantate was flash-evaporated, and the resulting red oil was dried *in vacuo* at 70 °C for several days.

Spectroscopic purity: ϵ(tailed)/ϵ(tailless) = 0.94. Anal. Calcd for $C_{94}H_{144}Cl_2N_6O_{44}Ru$: C, 50.54; H, 6.50; N, 3.76. Found: C, 48.34; H, 6.18; N, 4.14. Proton NMR in $CDCl_3$ (7.24 ppm): δ 3.33 s (12H), 3.51 t (8H), 3.60 s (88H), 3.81 t (8H), 4.52 t (8H), 7.55 t (2H), 7.81 d (2H), 8.05 m (10H), 8.39 d (2H), 8.91 s (4H).

[Ru(bpy(CO$_2$MePEG350)$_2$)$_3$](ClO$_4$)$_2$: 6-Tail Complex. A modification of the synthesis for [Ru(bpy(CO$_2$Et)$_2$)$_3$](ClO$_4$)$_2$ was used.[30a] To a 5 mL ethanol solution of bpy(CO$_2$MePEG350)$_2$ (0.62 g; 0.68 mmol) was added [Ru(dmso)$_4$Cl$_2$] (0.10 g; 0.21 mmol). The yellow slurry was refluxed under argon for 1 week. A green-black solution formed which slowly became red-brown. Flash evaporation led to an oil, which was chromatographed on a short silica column, eluting with DMF. A main orange band was separated from a briskly eluting green impurity and a sluggishly eluting orange-red impurity. Flash evaporation gave an oil, which was redissolved in $CHCl_3$ (10 mL; Mallinckrodt AR), and the solution was filtered to remove silica. The filtrate was flash-evaporated and dried at 70 °C *in vacuo* for several days, yielding an orange-red wax.

The chloride counterion was replaced by perchlorate in an aqueous titration using $AgClO_4$. The end point was monitored by Ag^+/Ag stripping wave voltammetry, in which the potential of a 25 μm diameter platinum electrode was cycled at 100 mV/s between 0.4 and −0.5 V versus SCE. The end point was signaled by the disappearance of the Ag^0 stripping wave at around 0 V.

Spectroscopic purity: ϵ(tailed)/ϵ(tailless) = 1.07. Anal. Calcd for $C_{126}H_{204}Cl_2N_6O_{34}Ru$ (chloride salt): C, 53.31; H, 7.24; N, 2.96. Found: C, 51.36; H, 6.99; N, 3.11. Proton NMR (chloride salt) in $CDCl_3$ (7.24 ppm): δ 3.15 s (18H), 3.32 s (12), 3.42 s (132H), 3.62 s (12H), 4.34 s (12H), 7.85 s (6H), 8.33 s (6H), 8.72 s (6H).

[Ru(bpy)$_2$(4,4′-bis(methoxycarbonyl)-2,2′-bipyridine)](NO$_3$)$_2$: Ester Analog of the 2-Tail Complex. This compound was unexpectedly formed by trans-esterification during an attempt to make the 2-tail complex. To a deoxygenated solution of [Ru(bpy)$_2$Cl$_2$] (0.10 g; 0.21 mmol) in 5 mL of methanol (Fisher Optima) was added $AgNO_3$ (0.065 g; 0.38 mmol; Baker). After 5 h of stirring under argon, the mixture was filtered to remove AgCl. A solution of bpy(CO$_2$MPEG350)$_2$ (0.18 g; 0.19 mmol) in 5 mL of methanol was added to the red filtrate. Refluxing under argon for 16 h gave a yellow-red solution. Flash evaporation led to an oil, which was redissolved in 5 mL water, and the solution was filtered to remove a gray-black impurity. The filtrate was flash-evaporated to an oil, from which crystallized a black solid, coated with a colorless liquid suspected to be the polyether. This liquid was washed away using Et_2O. The black solid was recrystallized from a minimum of methanol by dropwise addition of Et_2O. Brown, cubic crystals, which precipitated from the mixture, were isolated by filtration, washed with 25% methanol−Et_2O, Et_2O and hexanes, and air-dried.

Anal. Calcd for $C_{34}H_{28}N_8O_{10}Ru$: C, 50.43; H, 3.49; N, 13.84. Found: C, 48.38; H, 3.31; N, 13.29. Proton NMR in D_2O (4.61 ppm): δ 3.88 s (6H), 7.25 q (4H), 7.58 d (2H), 7.65 d (2H), 7.70 d (2H), 7.91 m (6H), 8.39 d (4H), 8.96 s (2H).

[Ru(bpy)(bpy(CO$_2$Et)$_2$)$_2$](ClO$_4$)$_2$: Ester Analog of the 4-Tail Complex. Bipyridine (0.022 g; 0.13 mmol) and $AgNO_3$ (0.044 g; 0.26 mmol) were added to a solution of [Ru(bpy(CO$_2$Et)$_2$)$_2$Cl$_2$] (0.10 g; 0.13 mmol) in 3 mL of PC. The mixture was stirred at room temperature for 16 h, causing a color change from blue-green to purple-red to orange-red. The mixture was poured into 100 mL of Et_2O, and the resultant mixture was swirled. The Et_2O−PC layer was decanted from the dark brown oily product, which was washed with 50 mL of Et_2O and resuspended in 5 mL water. Then the suspension was filtered to remove AgCl. To the filtrate was added 1 mL of aqueous of $NaClO_4 \cdot H_2O$ (0.04 g; Fisher). The resulting brick-red precipitate was isolated by filtration and washed with dilute aqueous $NaClO_4$ and cold water. The precipitate was recrystallized from 10 mL of 50% methanol−water by slow evaporation. The resulting red needles were collected by filtration, rinsed with cold water and Et_2O, and air-dried.

Anal. Calcd for $C_{42}H_{40}Cl_2N_6O_{16}Ru$: C, 47.74; H, 3.82; N, 7.95. Found: C, 49.69; H, 3.59; N, 7.93. Proton NMR in CD_3CN (1.93 ppm): δ 1.39 m (12H), 4.42 q (8H), 7.40 t (2H), 7.65 d (2H), 7.85 m (8H), 8.10 t (2H), 8.51 d (2H), 9.02 s (4H).

[Ru(bpy(CO$_2$Et)$_2$)$_3$](PF$_6$)$_2$: Ester Analog of the 6-Tail Complex. According to a modified synthesis of Elliott et al.,[30a] a 10 mL argon-purged ethanol suspension of [Ru(dmso)$_4$Cl$_2$] (0.20 g; 0.41 mmol) and bpy(CO$_2$Et)$_2$ (0.56 g; 1.86 mmol) was refluxed for 1 week, forming initially a brown solution, then a black suspension, and finally a red-brown solution. The mixture was cooled and filtered to remove excess ligand, and the filtrate was flash-evaporated. The residue was redissolved in 15 mL of water, and the solution was filtered to remove a gray impurity. To the red filtrate was added 5 mL of aqueous NH_4PF_6 (0.15 g; 0.91 mmol; Aldrich). The resulting orange-red precipitate was isolated by filtration and washed with cold water. Recrystallization by slow evaporation from 15 mL of acetone and 5 mL of water yielded product crystals, which were isolated by filtration, washed with cold water, and air-dried.

Anal. Caldd for $C_{48}H_{48}F_{12}N_6O_{12}P_2Ru$: C, 44.63; H, 3.74; N, 6.50. Found: C, 44.05; H, 3.50; N, 6.45. Proton NMR in acetone-d_6 (2.31 ppm): δ 1.64 t (18H), 4.72 q (12H), 8.23 d (6H), 8.63 d (6H), 9.62 s (6H).

Density Measurements. Room-temperature densities of the tailed complexes were obtained by suctioning the viscous liquids (with warming to reduce viscosity) into a preweighed 1 μL capillary (Drummond MicroCaps), using a syringe fitted with an adapter.

Differential Scanning Calorimetry (DSC). Samples (∼15 mg) were heated in Al pans at 70 °C *in vacuo* for 24 h before being sealed under dry nitrogen. Measurements were taken with a Seiko DSC220CU differential scanning calorimeter, scanning at 10 °C/min from +70 to −100 to +70 °C. Glass transition temperatures, T_G, are taken as the midpoint of the DSC sigmoids observed on the heating cycle,[35] and the change in heat capacity at T_G is taken from the difference between the plateaus of the sigmoid.

Viscosity. Measuring the very large viscosities of the [Ru(bpy)$_N$(bpy(CO$_2$MePEG350)$_2$)$_{3-N}$](ClO$_4$)$_2$ melts was a challenge owing to the small quantities available and their ready contamination with water. The capillary viscometry technique described by Flory[36] was used, in which the melt was sucked, under a pressure difference, Δp, from a small pool into a capillary (10 μL, Drummond Van-Lab). The time t, required to fill a segment of capillary (delimited by distances x_0 and x_1 from the submerged end) is

$$t = \frac{4\eta}{\Delta p r^2}(x_1^2 - x_0^2) \qquad (4)$$

where η is viscosity and r the capillary radius. The linear η *vs* t calibration plot used in the measurements of the ruthenium complex melts was derived for the capillary viscometer, using caramelized sucrose−glycerol solutions whose viscosities were determined with a cone-plate rheometer (Brookfield digital viscometer, Model DV3, CP52 cone). The capillary method, in principle, applies only to Newtonian fluids; shear rate independent cone-disk viscosity measurements do indicate that the 4-tail complex is Newtonian, and this is assumed to be true of the other Ru complex melts.

Ionic Conductivity. Ac impedance spectra (0.1−500 kHz) were obtained on a Schlumberger Model 1287 electrochemical interface and a 1260 impedance/gain phase analyzer. Microlithographically fabricated Pt interdigitated array electrodes (IDA),[37] having 100 fingers of 2 or 5 μm widths, 2 mm lengths, 0.1 μm heights, and 3 μm gaps, were coated with 3−5 mg of Ru melt. The melt-coated IDA was mounted on a home built stage[1b] using heat conductive paste (Buehler 0.05 μm alumina suspended in DOW-Corning high-vacuum grease) and was heated at 70 °C *in vacuo* (<30 mT) for 24 h and then cooled in 10 °C increments for recording the temperature dependence of the impedance spectrum. Ionic conductance was calculated from the semicircle of the spectrum.

Voltammetry in Dilute Solutions. Cyclic voltammetry was performed in deareated acetonitrile/0.1 M Bu_4NPF_6 (Fluka) in a Schott

(35) Angell, C. A. *J. Non-Cryst. Solids* **1991**, *131*, 13.
(36) Flory, P. J. *J. Am. Chem. Soc.* **1940**, *62*, 1057.
(37) The IDA (donated by Nippon Telephone and Telegraph) has a Si substrate with SiO_2 overlayer; masking around the fingers was with a silicon nitride insulating layer. The IDA cell was calibrated for ionic conductivity measurements using a LiCl−poly(propylene glycol) solution of known conductivity.

vial cell using Pt disk (0.47 mm diameter) working, Pt wire counter, and (fritted) aqueous Ag/AgCl/0.1M NaCl reference electrodes and a ferrocene (Fc) internal reference couple. Potentials are reported *vs* SCE, taking the Fc^+/Fc couple as 0.425V *vs* SCE.[38] Exact solution concentrations were determined from electronic spectra. A home built potentiostat and linear potential sweep generator were used.

Voltammetry in Undiluted Ru Complex Melts. Cyclic voltammetry of the undiluted Ru melts was performed with a home built potentiostat, using an IBM-compatible computer equipped with a Datel 412 analog IO board to provide linear sweeps. A polished epoxy disk platform, housing three exposed wire tip electrodes (a 6.3 μm radius Pt microdisk, a 0.25 mm radius Pt counter electrode, and a 0.25 mm radius Ag quasireference electrode)[39] was coated with 10−15 mg of Ru melt and heated to 70 °C under vacuum for 24 h before performing voltammetry. To record voltammetry as a function of temperature, the thermocouple-monitored temperature was lowered in 10 deg increments, allowing 10 min for equilibration. Self-diffusion coefficients were obtained by comparing voltammetric peak potentials and currents to digitally simulated cyclic voltammograms (Digisim),[40] assuming a reversible couple and accounting for uncompensated *iR* using the measured ionic conductivities.

Electronic Spectra. Electronic spectra of acetonitrile solutions were obtained in 1 cm quartz cuvettes on a Unicam UV-4 spectrometer.

Acknowledgment. This research was supported by grants from the Department of Energy and the Office of Naval Research.

Supporting Information Available: An activation plot and tables of formal potentials and electronic spectral data (3 pages). Ordering information is given on any current masthead page.

IC9706111

(38) Gennett, T.; Milner, D. F.; Weaver, M. J. *J. Phys. Chem.* **1985**, *89*, 2787.
(39) Watanabe, M.; Wooster, T. T.; Murray, R. W. *J. Phys. Chem.* **1991**, *95*, 45.
(40) Bioanalytical Systems, Lafayette, IN.